Rigid Block Distinct-Element Modeling of Dry-Stone Retaining Walls in Plane Strain

Mary Claxton[1]; Robert A. Hart[2]; Paul F. McCombie[3]; and Peter J. Walker[4]

Abstract: A simplified rigid block distinct-element numerical model is used to investigate the instability of dry-stone masonry retaining walls in plane strain. The investigation initially concentrates on modeling previously reported experimental data of wall behavior and thereafter assesses the influence of parametric variation on stability. Influence of masonry characteristics (wall joint shear stiffness, normal stiffness, tensile strength, and block geometry), backfill properties, and overall wall geometry are considered. Results from the experimental study and numerical model are compared with a limit equilibrium analysis.

DOI: 10.1061/(ASCE)1090-0241(2005)131:3(381)

CE Database subject headings: Retaining walls; Stones; Blocks; Plane strain; Numerical models.

Introduction

Dry-stone walling is an ancient and widely distributed form of wall construction, found wherever there is a plentiful supply of the basic raw materials. Historic and contemporary examples of free-standing enclosure walls, retaining and facing walls, and simple loadbearing buildings can be found in North and Latin America, Europe, Africa, Asia, and Australasia. Criss-crossing field walls are characteristic of many rural landscapes. Notable examples of dry-stone construction include Great Zimbabwe National Monument in Zimbabwe. Their widespread use stems from the abundant supply of raw materials combined with the success of a simple yet flexible and durable form of construction.

Walls are built by skilled masons through a careful process of selection and stacking, without the use of mortar, uncut and largely undressed stone rubble blocks. Stones are generally left rough except for occasional dressing using a hammer to remove unwanted edges. Suitable materials vary from sedimentary rocks such as limestone and sandstone, to harder igneous rocks of granite and basalt, and metamorphic rocks such as slate. Though block mass ranges typically between 5 and 20 kg, sizes can vary between stones less than 1 kg to massive rocks of a few tons.

For the construction of "engineered" retaining walls, dry-stone construction has largely been superseded by more modern techniques, such as reinforced concrete, reinforced earth, and gabion construction, but it remains a contemporary form of construction along hill roads in India (Arya and Gupta 1983) and elsewhere. Though a few new projects have recently been completed in the United States, for example, in the main it is the problems associated with the maintenance and assessment of existing dry-stone structures that professional engineers most commonly encounter. Throughout the industrial revolution a very large number of dry-stone retaining walls, varying in height from less than 1.5 m to over 15 m, were built as part of new transport networks across Europe. A number of dry-stone walls were also built in the eastern U.S. states within this period. Over a century later estimates of the length of walling still in-service along U.K. highways are conservatively placed at around 10,000 km, with a replacement bill in excess of £10 billion (O'Reilly et al. 1999). Many walls continue to perform quite satisfactorily, though they commonly fail to meet the safety criteria of modern design standards (BSI 1994).

Numerical stability assessment of existing walls is often complicated by out-of-plane deformations, such as bulging and leaning, together with poor understanding of the extent of cross section effective at resisting destabilizing forces and a lack of knowledge of backfill properties behind the wall. At present, the limiting deformations dry-stone walls can safely accommodate, without immediate fear of collapse, remain largely unknown and certainly vary from case to case. Consequently, assessment of structural integrity is still largely based on qualitative judgments following visual inspections (Highways Agency 1997). This limited understanding of wall behavior, combined with the inadequacies of current assessment techniques, exacerbates an increasing maintenance problem for highway authorities, faced with a large number of aging and distressed walls and an increasing rate of deterioration in recent years.

Objectives and Scope

Over the past 10–12 years the distinct-element method has been used with some success to model the stability of dry-stone walls (Dickens and Walker 1996; Wong and Ho 1997; Harkness et al. 2000). In this paper, the universal distinct-element code (UDEC),

[1]Graduate Engineer, The Morton Partnership Ltd., The Old Cavalier, 89 Dunbridge St., Bethnel Green, London, E2 6JJ, U.K.

[2]PhD Student, School of Chemical, Environmental, and Mining Engineering, Univ. of Nottingham, University Park, Nottingham, NG7 2RD, U.K.

[3]Dept. of Architecture and Civil Engineering, Univ. of Bath, Bath, BA2 7AY, U.K. E-mail: p.walker@bath.ac.uk

[4]Dept. of Architecture and Civil Engineering, Univ. of Bath, Bath BA2 7AY, U.K.

Note. Discussion open until August 1, 2005. Separate discussions must be submitted for individual papers. To extend the closing date by one month, a written request must be filed with the ASCE Managing Editor. The manuscript for this paper was submitted for review and possible publication on January 8, 2003; approved on April 7, 2004. This paper is part of the ***Journal of Geotechnical and Geoenvironmental Engineering***, Vol. 131, No. 3, March 1, 2005. ©ASCE, ISSN 1090-0241/2005/3-381–389/$25.00.

a two-dimensional (2D) distinct element package, has been used to model instability of dry-stone retaining walls. Initially the study concentrates on modeling results of early published experimental studies and thereafter assessing the influence of parametric variation on wall behavior. The influence of masonry joint characteristics (shear stiffness, normal stiffness, and tensile strength), backfill properties, wall block geometry, and overall wall geometry are considered in the investigation. Experimental and numerical behaviors are compared with a simple limit equilibrium analysis. In conclusion, the paper outlines recommendations for the use of UDEC to model masonry retaining wall stability, implications, and proposals for simplified stability checks, and suggestions for further research in this area.

Brief Overview of Dry-Stone Wall Engineering

Dry-Stone Wall Construction

The typical cross section of dry-stone retaining wall comprises one outer face of "coursed" stone blocks behind which there is a random core of more varied sized stones. Walls have generally been built with very shallow footings. Depending on the material used and quality of work, the proportion of voids in the wall is generally estimated to be between 10 and 20%, though voidage has been measured by the writers at 50%. The undressed blocks are typically randomly shaped, depending on the nature of the original deposit and subsequent weathering. Quarried materials for dry-stone walling are typically poor quality, as the finer quality materials are used for dimensioned stone masonry elements.

Walls are generally built with the front face battered backwards at between 1:5 and 1:10, improving the stability against overturning by moving the center of gravity backwards, compared with a vertical front face. While the back face of the wall may be ill defined, with rubble merging into the backfill, the back often leans back less than the front, producing a tapered section, which makes a more efficient use of walling material. Fill behind retaining walls, often including construction waste, was typically poorly compacted during initial construction. Its subsequent settlement is widely believed to be a significant contributory factor to later wall deformation and instability. For walls built in front of clay bearing deposits, the initial negative pore water pressures that developed following excavation have subsequently been lost over time, resulting in a progressive loss of tensile strength and reduction in shear strength. This slow process is also believed to make a significant contribution to recent increases in the perceived rate of wall collapse and deterioration as the timescale involved for large retaining structures may be over 100 years. Such structures have been standing on the basis of temporary strength, and become unstable as pore pressures reach temporary equilibrium. The presence of significant vegetation can prolong this process, sometimes indefinitely, by maintaining long-term negative pore pressures. However, the common presence of reasonably free-draining crushed stone behind many collapsed walls indicates that this is by no means always the case.

Wall Behavior

As gravity earth retaining structures, dry-stone walls are often assumed for purposes of simple stability analysis to behave in the same manner as rigid masonry and mass concrete structures. However, dry-stone walls are not rigid structures, but can sustain considerable leaning or bulging deformation for a number of years without collapse. Out-of-plane deformations in the order of 50 mm are generally not considered significant. Rigid stability analysis, based on dimensions of the masonry face, has repeatedly shown that these walls often lack the proportions required to maintain an acceptable factor of safety to prevent toppling or sliding failure required by modern design codes (Jones 1979, 1990; O'Reilly et al. 1999). However, because of the irregular and graded form of construction, comprising a rubble fill behind the masonry face, a significant problem faced by assessors is one of determining the section thickness actually effective in resisting backfill pressures.

Wall deterioration and eventual failure may be attributed to many causes, including buildup of water pressure following mortar pointing, settlement of poorly compacted fill or foundations, poor quality materials and construction, weathering of stone, effects of new construction work, inappropriate earlier repairs, vehicular impact and vegetation growth (Walker and Dickens 1995; Cooper 1986). Influences of new construction works include altering water drainage, failure of adjacent service pipes and excavation of service trenches in front of the wall for example. Monitoring of retaining walls in Zimbabwe has demonstrated close correlation between movement and seasonal rainfall (Walker and Dickens 1995). Similarly, records of 48 unattributed retaining wall collapses in Gloucestershire, U.K., between 1981 and 2000, show that 73% of failures occurred during fall and winter months, when ambient soil moisture contents are characteristically higher. Increasing soil moisture reduces any soil suction that may be present, so reducing soil shear strength, and may be sufficient to produce positive pore water pressures, which will also act directly on the back of a retaining structure which has lost its initial permeability.

Previous Engineering Studies

In stark contrast to their widespread use, there have been very few engineering studies of dry-stone earth retaining walls. The Royal Engineers undertook the first experimental investigations over 150 years ago. In two separate studies full-scale dry jointed retaining walls were built in progressive stages, and their response to backfill pressures noted (Corps of Royal Engineers 1845; Burgoyne 1853).

In 1834, Lieut-General Burgoyne built four full-scale granite dry-stone walls in a disused quarry in Ireland. Each wall was 6.1 m long and 6.1 m high (Fig. 1). Though wall cross sections varied, the average wall thickness remained constant at 1.02 m (approximately one-sixth the height). Walls "A" and "D" were built with uniform thickness; wall A had a constant inward batter of 1 in 5, while wall D was vertical. Walls "B" and "C" had thickness varying from 1.626 m at the base to 0.406 m at the top; wall B had a vertical back face, while wall C had a vertical front face. Each wall was backfilled with soil, placed in 0.61 m lightly compacted layers, and its condition was noted after each stage. Walls A and B reached full height, though some outward displacement was noted. However, walls C and D both collapsed when the backfill height reached 5.2 m high. Remarkably Burgoyne's investigation remains the most detailed full-scale experimental work on dry-stone retaining walls carried out to date.

Walker and Dickens (1995) have reported on the appraisal and conservation of dry-stone wall structures at Great Zimbabwe National Monument. During this work they pioneered the use of the distinct-element method (Cundall 1971) to model stability analysis of free-standing and retaining dry-stone walls (Dickens and Walker 1996). Using a relatively simple UDEC model they were

Wall	Description	Section profile
A	Leaning wall: opposite sides equal and parallel. Wall height: 20 feet (6.1 m) Uniform thickness: 3 feet 6 inches (1.02 m) Wall batter: 1 in 5 Backfill height: 20 feet (6.1 m)	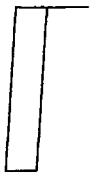
B	Sloping wall. Wall height: 20 feet (6.1 m) Thickness at base: 5 feet 4 inches (1.626 m) Thickness at top: 1 foot 4 inches (0.406 m) Mean thickness: 3 feet 6 inches (1.02 m) Wall batter to front face: 1 in 5 Backfill height: 20 feet (6.1 m)	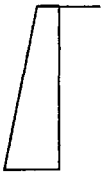
C	Counter sloping wall. Wall height: 20 feet (6.1 m) Thickness at base: 5 feet, 4 inches (1.626 m) Thickness at top: 1 foot 4 inches (0.406 m) Mean thickness: 3 feet 6 inches (1.02 m) Wall batter to back face: 1 in 5 Backfill height 17 feet (5.2 m) at failure	
D	Rectangular wall. Wall height: 20 feet (6.1 m) Uniform thickness: 3 feet 6 inches (1.02 m) Backfill height: 17 feet (5.2 m) at failure	

Fig. 1. Burgoyne's test walls

able to simulate bulging deformations observed during full-scale tests. Subsequently other investigators have applied the technique to retaining walls (Wong and Ho 1997). Harkness et al. (2000) have used UDEC successfully to simulate numerically Burgoyne's test walls; expanding on this work, they have more recently considered deformation and failure modes in dry-stone retaining walls (Powrie et al. 2002). In this work, wall failure mode and deformations subject to increasing depth of backfill are shown, by 2D numerical distinct element modeling, to be a function of stiffness and strength of block joints and backfill material.

Distinct Element Modeling

General Description of Model

The distinct-element method, first presented thirty years ago by Cundall (1971) to model jointed rock masses subjected to either static or dynamic loading, was used to model the dry-stone retaining walls. The distinct element method has been developed over the past 30 years for modeling discontinuous media, such as jointed rock masses, under static or dynamic loads. The discontinuous media is represented by a series of discrete blocks. Discontinuities, or joints, are represented as boundary conditions between the blocks.

Blocks may be defined as rigid, as such all displacements within the media result from normal and shear displacements at boundaries between the blocks. Alternatively, deformable blocks are split into a mesh of finite difference elements which may be assigned linear or nonlinear force displacement relations for both normal and shear stresses. Joint normal and shear deformations at boundaries between adjacent blocks are assigned either linear or nonlinear force-displacement relations. Large displacements along joints are permitted by the distinct-element model.

The UDEC (version 3.0), a 2D distinct element model, was used throughout for this study (Itasca Consulting Group 1996). Contact forces and displacements at interfaces are determined through a series of calculations tracing movement of the blocks with increasing time increments. Movements are caused by propagation of applied loads and body forces through the system. The solution is a dynamic process represented by a time-stepping algorithm. Calculations alternate between application of contact force-displacement laws and Newton's second law of motion. Interface force-displacement relations define contact forces, and Newton's law gives block motion arising from known contact forces. Contact points are automatically updated as the blocks move. Similar to dynamic relaxation, static problems are readily analyzed by allowing the dynamic model to reach equilibrium. Equations of motion are damped, using velocity-proportional damping, to reach force equilibrium as quickly as possible.

UDEC version 3.0 is supported by *FISH*, an in-built programming language allowing the user to define specific functions. A variety of body and joint constitutive models are available, including an elastic Mohr–Coulomb plastic material model, which was used for the soil backfill. Material characteristics are user defined and, where appropriate, readily modified using *FISH* as the analysis proceeds.

The numerical dry-stone wall model is defined by a number of material properties assigned to the blocks and joints. Some material property terms used in this study are briefly defined below:

1. Joint properties:
   - *Normal stiffness*: The ratio between normal (compressive) stress and normal strain across a joint;
   - *Shear stiffness*: The ratio between shear stress and shear strain acting along a joint;
   - *Angle of friction*: The natural angle of repose along a joint between two materials at which frictional resistance is overcome; and
   - *Tensile strength*: Normal tensile resistance of a joint between two materials (often assumed zero).
2. Deformable material properties:
   - *Shear modulus* (G): The ratio between shear stress and shear strain for a material. For an elastic model shear modulus is given by $G=E/2(1+\nu)$;
   - *Bulk modulus* (K): The ratio of volumetric stress to volumetric strain. For an elastic model bulk modulus is given by $K=E/3(1-2\nu)$; and
   - *Angle of friction*: internal angle of frictional resistance for a material.

Numerical Model Details

Recently Harkness et al. (2000) reported on a distinct-element model simulation of Burgoyne's experimental investigation. Based on UDEC version 2.0, Burgoyne's original experimental observations were successfully reproduced: Walls A and B remained stable, while walls C and D collapsed at the appropriate fill height. Wall blocks, soil backfill, and rock base material were analyzed using a 2D plane strain distinct element model, comprised of deformable blocks and a mesh of 6,427 elements. The wall, soil, and rock base were modeled as elastic-Mohr–Coulomb plastic materials, with properties outlined in Table 1. Pore water pressures were assumed zero throughout. Each numerical analysis took up to seven days on an RS6000 workstation.

Using UDEC version 3.0, the investigation described here ini-

Table 1. Material Characteristics (Harkness et al. 2000)

Property	Wall	Soil
Unit weight	22.7 kN/m^3	15.5 kN/m^3
Bulk modulus	22,000 MPa	Linear variation with depth between 1 MPa (top) and 10 MPa (base).
Shear modulus	15,000 MPa	Linear variation with depth between 0.6 MPa (top) and 6.6 MPa (base).
Internal angle of friction	45°	28°
Joint normal stiffness	1,000 MPa/m	
Joint shear stiffness	500 MPa/m	
Joint angle of friction	45°	

tially sets out to simulate Burgoyne's experimental results and compare findings with those reported by Harkness et al. (2000). Thereafter, the influence of physical and numerical parameters on simulated wall behavior was investigated. Findings described in this paper are part of an on-going investigation of dry-stone wall behavior.

A 2D plane strain model was selected for the analysis. The 51 wall blocks were taken as rigid, while the soil was a deformable block comprised of 3,337 elements with elastic-Mohr–Coulomb plastic properties. Rigid wall blocks were adopted to simplify the numerical model and reduce run times compared with those reported for previous simulations. Defining the wall material using rigid block elements, however, limits the stress information which can be obtained along block joint interfaces. In the original experiments, the walls were built on a rigid granite base (Burgoyne 1853) and the UDEC numerical model reflects this condition. However, the base material was defined as deformable beneath each wall in order to investigate the distribution of basal pressures, Fig. 2. Base material values adopted were the same as for the granite wall material shown in Table 1. The deformable base was limited to beneath the wall as this is the zone of most interest and it optimizes run times by limiting the total number of deformable blocks in the model. In keeping with the original construction of Burgoyne, the soil was added in 0.61 m (2 ft) layers to a full height of 6.1 m, or that necessary to cause collapse of the wall. As a benchmark material properties were taken as outlined in Table 1. However, once the model was validated, in terms of stability, material characteristics were systematically varied, Table 2, to study their influence on wall behavior.

The material properties outlined in Table 1, including wall and joint angle of friction and joint stiffness values, were those used by Harkness et al. (2000) and were based, as much as possible, on values originally reported by Burgoyne (1853). In the absence of direct experimental data, the joint properties (shear stiffness, normal stiffness, and friction angle) were derived by Harkness et al. (2000) through trial and error calibration of their deformable numerical model with the wall test results. Experimental values for noninterlocking joints between granite blocks report joint shear stiffness values around 100 MPa/m and joint normal stiffness around 200 MPa/m (Walker and Dickens 1995), much lower than those used by Harkness et al. (2000). A relatively high value of 45° for the joint shear stiffness and friction angle limits the likelihood of shear deformation. Earlier studies by Cooper (1986) had suggested that bulging in dry-stone walls develops through rotational rather than shear displacement between blocks. By initially maintaining such a high joint friction angle, the analysis seeks to investigate the relative significance of joint shear on the development of bulging in dry-stone walls. As large displacements are being modeled, the angle of dilation has been set as zero for both the backfill and the joints. The significance of material properties on behavior is further investigated during the parametric analysis.

Table 2. Variation of Material Parameters

Property	Wall	Soil
Unit weight (kN/m^3)	20,*22.7*,26	1,250,1400,*1,550*,1,700
Internal angle of friction	Not varied	22°,*28°*,34°
Joint normal stiffness (MPa/m)	200,500,*1,000*	
Joint shear stiffness (MPa/m)	100,300,*500*	
Joint angle of friction	20°,30°,*45°*,60°	
Joint tensile strength (MPa)	*0*,2	
Wall thickness (mm)	400,750,*1,000*	
Block thickness (mm)	100,200,*varied*	

Note: Figures in italics represent benchmark values.

Results and Discussion

Initial Simulations

The numerical model for Burgoyne's wall D is shown in Fig. 2. Using material parameter values set out in Tables 1 and 2, the simplified rigid block wall model successfully replicated Burgoyne's observed experimental behavior for all four walls; walls A and B were stable at a full backfill height of 6.1 m, whereas walls C and D collapsed when backfill reached 5.2 m. Horizontal displacement response at the top of the wall D during the addition of the final two soil layers is shown in Fig. 3. After the addition of each of the first eight layers, the deflection reaches a stable value once the numerical model attained equilibrium. Deflection of the wall on completion of layer eight was 22.6 mm, which compares reasonably well with 35 mm reported by Harkness et al. (2000). On addition of the ninth layer, the deflection response accelerated, indicating that the wall was collapsing by overturning, Fig. 4, as both block velocity and displacement increased with wall height above the base. At stable equilibrium, the calculated deflection at the top of wall B was 5.4 mm, which is significantly less than the 64 mm quoted by Burgoyne and the 32.6 mm reported for a deformable block model (Harkness et al. 2000).

The slight heave behavior predicted in the fill layers immediately behind the wall, Fig. 4, is a consequence of the large rotational deformation of the wall, backwall friction, and tensile strength developed by each fill layer. In practice, tensile failure of the fill is likely to occur, and in fact is quite commonly observed in deformed dry-stone walls prior to their collapse. The influence of this aspect of behavior is to be investigated further in future work.

Though the rigid block model in all four cases accurately simulated wall stability/instability, the model's stiffness generally exceeded both experimental and deformable model predicted values using the material properties used by Harkness et al. (2000) in their deformable model study. The rigid block model limits wall deformations to joint displacements between blocks. As such, it can be expected that the rigid block model will be stiffer than the deformable block model. Therefore, to study the effect of material properties, in particular joint stiffness, a parametric analysis was undertaken and results are discussed below.

Typically each numerical analysis took 60–80 min to run on a

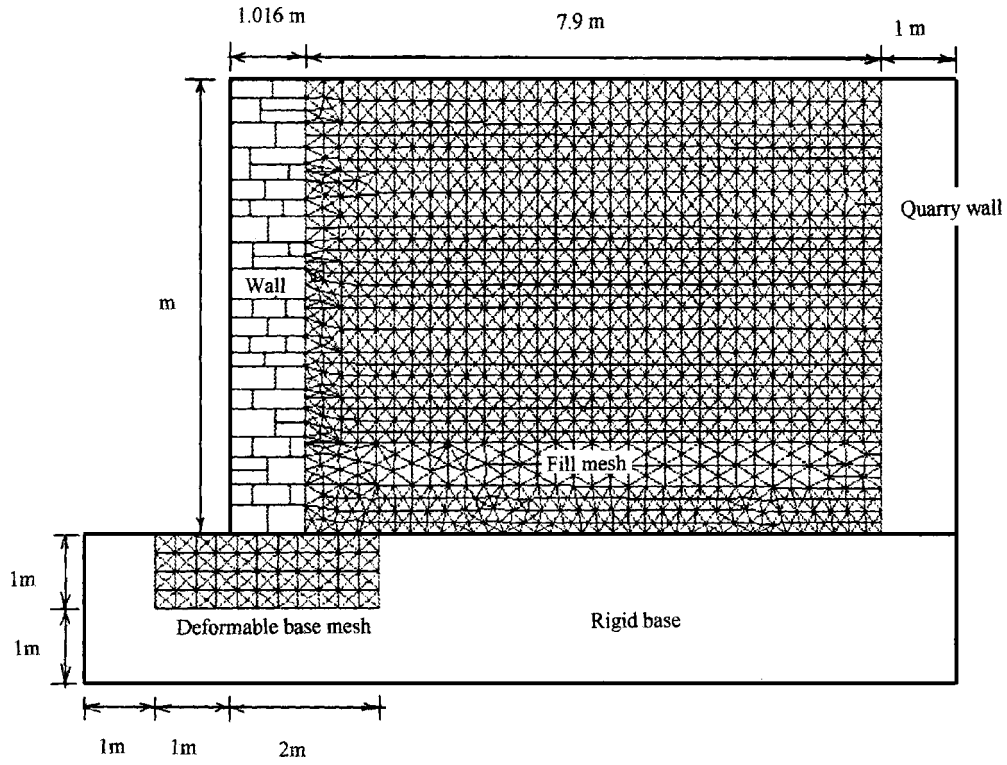

Fig. 2. Distinct-element model

Pentium II (333 MHz) desk-top personal computer. Once the wall had become unstable the run was often automatically terminated by UDEC for violating specified block overlap criteria during large deformations. Relaxing block overlap criteria allows greater overall displacements to be modeled but, as a general rule, reduces accuracy of the numerical model. The run times were significantly shorter than the seven days quoted by Harkness et al. (2000). Simplifying the model (rigid wall blocks and fewer soil elements), combined with an updated version of UDEC running on now quite modest hardware, allowed the analysis to be completed within a time span acceptable for routine wall assessment.

The normal stress distributions along the soil/wall interface, 2 m behind the wall face, and beneath the wall are given in Fig. 5. One consequence of using rigid blocks and a coarser soil mesh has been the expected downgrading in the accuracy of the computed stress data. In comparison with past work, the normal stress distribution along the soil/wall interface soils shows greater variation, though maximum and resultant magnitudes are in closer agreement. Horizontal stresses behind the wall face were also in general agreement with active pressures predicted by Caquot and Kérisel (1948).

Numerical collapse is typified by development of an active failure wedge defined by an inclined slip plane drawn from the toe or midbase of the wall rather than more classically the heel, Fig. 4. This form of failure is attributed to the flexible unbonded nature of the wall construction and is supported by observations

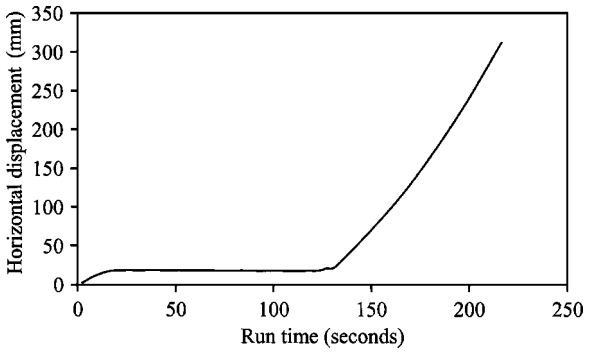

Fig. 3. Horizontal displacement response at the top of a wall during backfilling

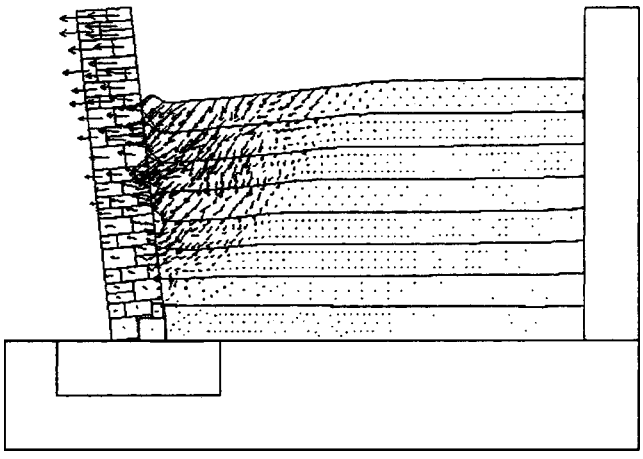

Fig. 4. Velocity vectors

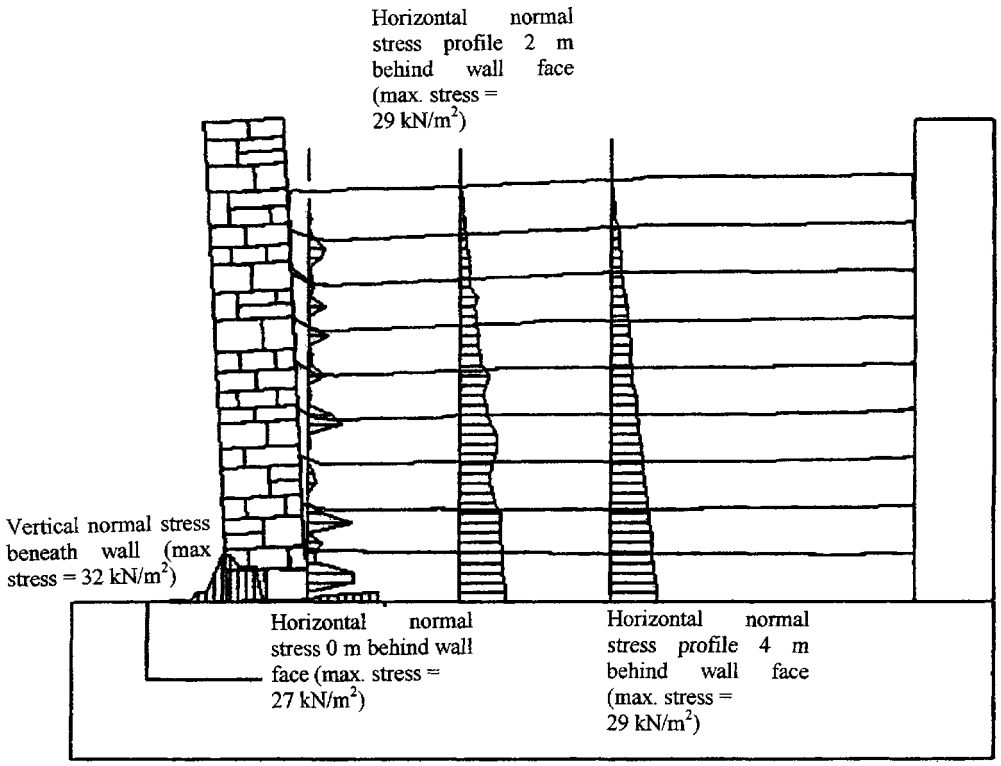

Fig. 5. Normal pressure plots at failure

of wall collapses. Though representing a significant reduction in the effective volume of material retained by the wall, the failure mode governs due to the corresponding reduction in restoring moment. It is a natural consequence of the mechanism of rotation about the toe, which leaves the blocks at the heel of the wall lying on the foundation. Were there a tensile connection between these blocks and the rest of the wall, the active wedge would be expected to terminate at the heel. It is the coursing of the blockwork that determines the termination of the active wedge.

Parametric Analysis

Results of the parametric numerical analysis are summarized in Table 3 below. Effects on wall stability, running time, wall displacement, and horizontal pressures are presented. Other performance data, such as normal stresses along the wall base and soil shear stresses, are readily available from the numerical model, but for brevity have not been included in Table 3. Wall failure mode (toppling failure) has been unchanged by the parametric variation, although the number of soil layers causing collapse and form of the active failure wedge did change.

Parametric variation had little significant impact on run time of numerical simulations. Where wall displacements significantly increased run times tended to increase as well, Table 3. Run times are governed by variety of parameters, including model resolution (number of blocks and number of mesh elements in deformable blocks), tolerances set for convergence and numerical damping, and specifications of the computer hardware. Increasing the number of deformable blocks and mesh fineness increases the number of computations and consequently has a significant impact on run times. As the parametric study was limited to a variation of material properties using the same basic model, it is can be reasonably expected that run times are generally little changed.

Changing wall joint normal and shear stiffness, over the range given in Table 2 had no effect on number of layers required to cause toppling failure, but displacement at the last stable layer increased in comparison with baseline data. Reducing joint normal stiffness in the wall had greatest impact on displacement, suggesting perhaps that stable wall displacements are governed by rotational, rather than sliding, movements between block layers. In one case, an 80% reduction in wall normal stiffness increased last stable layer displacement by over 700%, Table 3. Therefore, by refining joint stiffness properties, it is possible to reproduce accurately physical test performance using a simplified rigid block numerical model.

Varying unit weight of the wall blocks, in the range of $20-26\ \mathrm{kN/m^3}$, did not alter wall stability. However, stable displacements increased as unit weight decreased and, correspondingly, the predicted maximum lateral pressures behind the wall increased as wall deflection decreased. Reducing block height has had little impact on strength, though again displacements preceding failure increased by over 48% when block height was halved (Table 3). As the number of blocks and joints increased, as block height reduced, the expectation is for overall wall stiffness to decrease with an increasing number of joints in the wall structure.

Wall strength decreased with a reduction in wall thickness; failure mode was unchanged however. Ratio of soil depth at failure to wall thickness varied between 5.4 and 7.6, increasing for more slender walls. Increasing joint tensile strength to 2 MPa, though importantly not along the base, improved stability, as the wall was capable of withstanding an additional soil layer before collapsing. Wall stiffness also increased as deflection at the eighth soil layer decreased by 50% compared to the baseline run. This is an encouraging result for maintenance works as mortar pointing and grouting are common remedial interventions for distressed dry-stone walls.

Wall strength was also impaired by a reduction in joint friction

Table 3. Summary of Parametric Analysis

Parameter	Number of soil layers to cause failure	Time to complete last stable layer (n) (s)	Wall displacement at last stable layer (mm)	Maximum horizontal stress along soil/wall interface (kPa)
Unit weight (wall blocks)				
20 kN/m^3	9	147 (8)	28.1	28.2
22.7 kN/m^3	*9*	*133 (8)*	*22.6*	31.7
26 kN/m^3	9	112 (8)	21.5	32.5
Joint angle of friction in wall				
20°	8	135 (7)	35.7	25.6
30°	9	125 (8)	33.1	44.7
45°	*9*	*133 (8)*	*22.6*	31.7
60°	9	123 (8)	23.8	29.4
Joint normal stiffness in wall				
200 MPa/m	9	266 (8)	182.0	28.7
500 MPa/m	9	147 (8)	49.9	29.2
1,000 MPa/m	*9*	*133 (8)*	*22.6*	31.7
Joint shear stiffness in wall				
100 MPa/m	9	147 (8)	26.5	44.3
300 MPa/m	9	140 (8)	23.7	29.5
500 MPa/m	*9*	*133 (8)*	*22.6*	31.7
Joint tensile strength in wall				
0 MPa	*9*	*133 (8)*	*22.6*	31.7
2 MPa	10	116 (9)	11.3[a]	28.9
Wall block thickness				
100 mm	9	358 (8)	86.4	30.1
200 mm	9	127 (8)	58.1	29.2
Varied	*9*	*133 (8)*	*22.6*	31.7
Wall thickness				
400 mm	5	137 (4)	54.3	12.2
750 mm	7	173 (6)	93.4	21.5
1,016 mm	*9*	*133 (8)*	*22.6*	31.7
Fill internal angle of friction				
22°	8	126 (7)	22.8	24.7
28°	*9*	*133 (8)*	*22.6*	31.7
34°	10	189 (9)	19.8	32.9
Fill unit weight				
12.5 kN/m^3	9	139 (8)	17.2	21.8
14.0 kN/m^3	9	144 (8)	19.4	25.5
15.5 kN/m^3	*9*	*133 (8)*	*22.6*	31.7
17.0 kN/m^3	9	156 (8)	28.7	30.7

Note: Figures in italics represent the benchmark values.

[a]Stable wall deflection after eight soil layers.

angle. The toppling failure mode, and strength, appears relatively insensitive to significant changes in wall friction angle. For changes in the friction angle of ±15° stable wall height is unchanged. Reducing wall friction angle to 20° reduced stable height by one layer, but failure mode remained as toppling rather than changing to sliding failure for lower joint friction angles. Deflection at the last remaining stable layer increased as the wall joint frictional strength decreased.

In line with expectations, increasing or reducing soil strength resulted in a corresponding increase or reduction in soil height necessary to induce wall failure. However, varying soil unit weight had little effect on wall strength, though both wall displacement and horizontal pressures varied with corresponding changes in soil unit weight, Table 3. Predicted behavior of wall strength is, however, consistent with accepted soil mechanics theory.

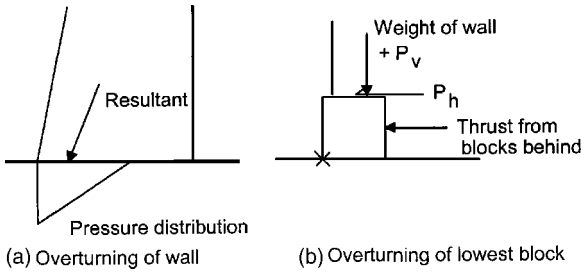

Fig. 6. Conditions for overturning failure

A limit equilibrium analysis was carried out to investigate the stability of each wall, using Coulomb earth pressure coefficients, in a specially written small computer program. The assumed angle of friction of 28° was used as a starting point. This indicated the factor of safety against the masonry walls sliding forward was well over 1.0 in every case. However, the resultant force acted outside the middle-third of the base for all the walls; consequently, the pressure distribution on the base of the walls was triangular rather than trapezoidal, and over less than the full width of the base [Fig. 6(a)]. As the position of the resultant moves forward over the base, the loaded width reduces, with the consequent stress increasing rapidly, until the entire load acts at the front of the base, and the wall overturns. This is shown in Fig. 6(a).

Before the wall as a whole overturns, it would normally be expected that a bearing failure would occur, or crushing of the wall material, but in this case all materials were granite and of high strength. In fact, because the blocks are not cemented, the lowest block in the wall will overturn before the entire wall overturns. The main overturning force comes from the horizontal component of earth pressure P_h, which will be carried entirely by friction on the top of this block, resulting in a moment about the toe of the block equal to P_h multiplied by the height of the block [Fig. 6(b)]. Resisting this will be the moment due to the vertical load, equal to the weight of the wall above plus the vertical component of earth pressure, P_v. P_h and P_v are obtained for the fill above the top of the block. The horizontal thrust transmitted from the blocks behind provides a small additional overturning moment.

Wall overturning and block overturning have been examined by considering the angle of friction necessary to just prevent these failure modes as the height of the fill is increased. Based on Burgoyne's drawings, the height of the lowest block is taken to be 0.305 m. Fig. 7 shows that only Wall D was at risk of overall overturning, with a fill height of just over 5.2 m being possible with $\phi = 28°$. For wall B, 6.1 m of fill only requires 15° angle of friction, and does not even appear on the plot. The other walls needed about 22° for the full 6.1 m height. Overturning of the wall therefore appears to be a possible failure mode for Wall D based upon $\phi = 28°$, but does not explain the failure of Wall C.

For overturning of the basal block, Fig. 8 shows Wall D only reaching 5.1 m with $\phi = 28°$, which given the precision of the data is in good agreement, while Wall C could not be expected to exceed 5.6 m. The drawings of the walls indicate that the filling was far from uniform, and this is probably sufficiently close

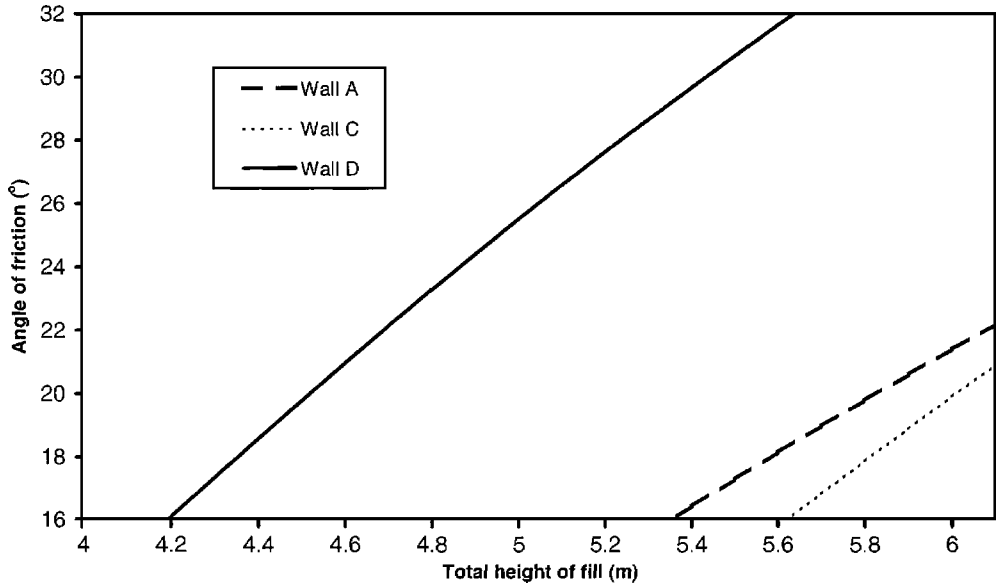

Fig. 7. Mobilized angle of friction to prevent overturning of entire wall

agreement to suggest that this mechanism explains the observed failures, and supports the use of $\phi = 28°$. It may also be noted that this mechanism appears to correspond to the failed cross sections reported by Burgoyne (1853).

Conclusions

A distinct-element numerical model, comprised of rigid wall blocks and deformable soil, has been used to successfully reproduce observed experimental wall behavior and earlier simulations. Limit equilibrium analysis was carried out to further investigate wall stability by exploring conditions necessary for wall and base block overturning.

Computation time for the simulations suggests that UDEC could, with further refinement, indeed prove to be a useful tool for the routine assessment of dry-stone walls. There is, of course, the need for further development to produce a generic model allowing systematic variation of parameters in analysis.

Failure mode of the wall was unchanged during extensive parametric analysis. Changing wall unit weight, joint stiffness characteristics, and block geometry had little effect on the stability, though precollapse deformations were often significantly altered. Stable height for the wall was improved by adding joint

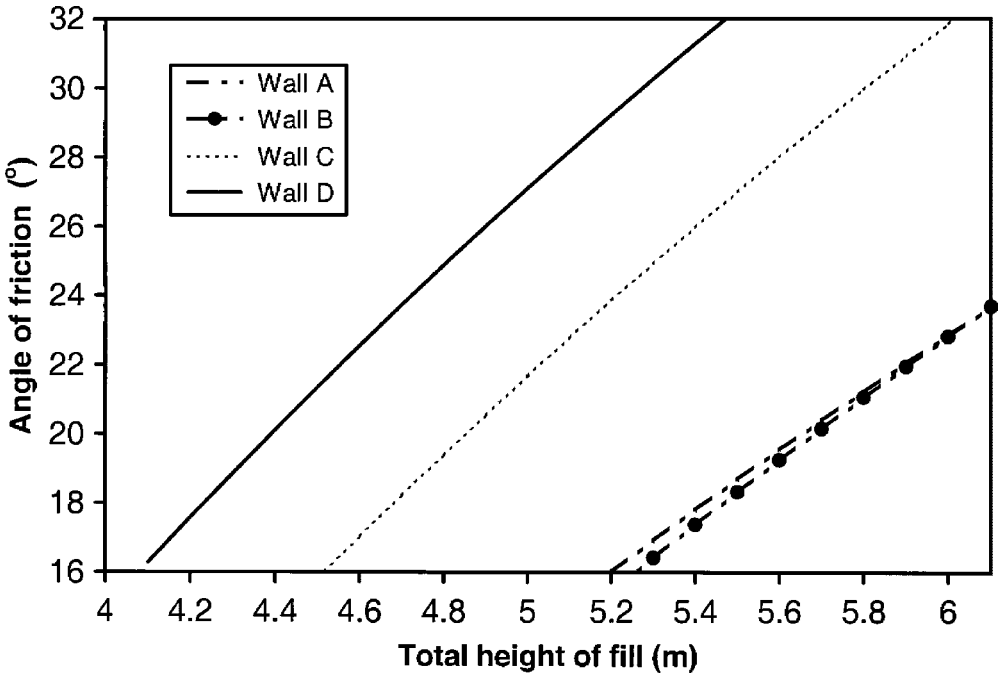

Fig. 8. Mobilized friction to prevent overturning of lowest block

tensile strength and, as expected, greatly influenced by wall thickness. The block joint friction angle also influenced stability, though failure mode remained toppling rather than sliding. Varying soil unit weight and strength also had the expected influence on wall stability.

Joint properties, in particular normal stiffness, had a significant effect on predicted wall displacement during the parametric study. Reducing joint normal stiffness decreased overall wall stiffness and so increased the last stable fill layer deformations. Through careful selection of material properties, and further calibration, a simplified rigid block model may be used to accurately predict precollapse deformations in flexible dry-stone walls.

Comparing numerical analysis with Burgoyne's tests has helped to validate the distinct-element model. Burgoyne's walls were, however, atypical construction, lacking the graded core commonly found behind the wall face. In addition, walls are often sited on soft rather than rigid foundations. The walls modeled to date have all failed by toppling, whereas the most significant maintenance problem remains bulging of the wall face. Further work is therefore currently on-going in which the influence of factors, such as form of construction, foundation type, and wall and soil properties on wall stability, are being considered.

Acknowledgments

The writers would like to acknowledge the support of the Engineering and Physical Sciences Research Council (GR/M31477), Gloucestershire County Council, Somerset County Council, and Wiltshire County Council for financing this work. In addition, they also thank colleagues at Southampton University for their advice and support.

Notation

The following symbols are used in this paper:

E = elastic modulus;
G = shear modulus;
h_s = height of backfill;
h_w = height of wall;
K = bulk modulus;
k_a = active pressure coefficient;
M_o = overturning moment;
M_R = restoring moment;
P = resultant lateral thrust on wall;
P_h = horizontal component of earth pressure;
P_v = vertical component of earth pressure;
t = wall thickness;
y = leverarm;
γ_s = unit weight of soil;
γ_w = unit weight of wall;
δ = angle of wall friction;
ν = Poisson's ratio; and
ϕ, Φ = soil internal angle of friction.

References

Arya, A. S., and Gupta, V. P. (1983). "Retaining wall for hill roads." *Indian Road Congress J.*, 44(1), 291–326.

British Standards Institution (BSI) (1994). "Code of practice for earth retaining structures." *BS 8002*, British Standards Institution, London.

Burgoyne, J. (1853). "Revetments or retaining walls." *Corps of Royal Eng.*, 3, 154–159.

Caquot, A., and Kérisel, J. (1948). "Tables for calculation of passive pressure, active pressure, and bearing capacity of foundations." Gaithier-Villars, Paris.

Cooper, M. R. (1986). "Deflections and failure modes in dry-stone retaining walls." *Ground Eng.*, 19(8), 28–33.

Corps of Royal Engineers. (1845). "Experiments carried on at Chatham by the late Lieutenant Hope, Royal Engineers, on the pressure of earth against revetments, and the best form of retaining walls." *Corps of Royal Eng.*, 7, 64–68.

Cundall, P. A. (1971). "A computer model for simulating progressive large-scale movements in blocky rock systems." *Proc., Symp. Int. Soc. Rock Mechanics*, Paper No. II-8.

Dickens, J., and Walker, P. (1996). "Use of distinct-element model to simulate behavior of dry-stone walls." *Struct. Eng. Rev.*, 8(2/3).

Harkness, R. M., Powrie, W., Zhang, X., Brady, K. C., and O'Reilly, M. P. (2000). "Numerical modeling of full-scale test on drystone masonry retaining walls." *Geotechnique*, 50, 165–179.

Highways Agency. (1997). "The assessment of highway bridges and structures." *BA 16*, The Stationary Office, London.

Itasca Consulting Group. (1996). *UDEC version 3.0 user manual*, Minn.

Jones, C. J. F. P. (1979). "Current practice in designing earth retaining structures." *Ground Eng.*, 12(6), 40–45.

Jones, C. F. J. P. (1990). "Dry stone walls." *The maintenance of brick and stone masonry structures*, E&FN Spon, London, 349–360.

O'Reilly, M. P., Bush, D. I., Brady, K. C., and Powrie, W. (1999). "The stability of drystone retaining walls on highways." *Proc. Inst. Civ. Eng. Municipal Eng.*, 133, 101–107.

Powrie, W., Harkness, R. M., Zhang, X., and Bush, D. I. (2002). "Deformation and failure modes of drystone retaining walls." *Geotechnique*, 52(6), 435–446.

Walker, P., and Dickens, J. (1995). "Stability of medieval dry stone walls in Zimbabwe." *Geotechnique*, 45(1), 141–147.

Wong, H. N., and Ho, K. K. S. (1997). "The 23 July 1994 landslide at Kwun Lung Lau, Hong Kong." *Can. Geotech. J.*, 34, 825–840.